*Bulletin de la Société Royale des Sciences de Liège, Vol. 88, Actes de Colloques, 2019, p. 44 - 49*

# Atomic diffusion across the HR diagram

Olivier Richard

Laboratoire Univers et Particules de Montpellier, Université de Montpellier, CNRS,
place Eugène Bataillon, 34095 Montpellier, France.

**Abstract:** It is clear that in order to explain many observed stellar phenomena, atomic diffusion must be included in stellar models. The effects of atomic diffusion are not limited to the surface abundances as we will see, it occurs in stars from the surface to the center and even if these effects are reduced in the external layers by other transport processes it remains in the center. We will also see that the induced chemical stratification has a strong impact on the stellar opacity.

**Keywords:** atomic diffusion – star:abundances – star:evolution – star:interiors

## 1 Introduction

With the advent of modern physics in the early twentieth century stellar physics took a new start. Even before the star energy source was known, many physical processes had been studied in stellar interiors like atomic diffusion, which is the relative movement between the different ions of the plasma due to the temperature, pressure and chemical gradients inside the star and to the interaction between ions and photons (see Michaud et al. 2015 for a detailed description). Atomic diffusion inside stars was already discussed in the pioneering works of Eddington (1916) and Chapman (1917). Atomic diffusion was then neglected in most of the studies until the work of Michaud (1970) which shows that radiative accelerations are responsible for the overabundances of many elements in peculiar A stars. Now it is well accepted that atomic diffusion plays a crucial role in a large variety of "chemically peculiar" stars. Helioseismology shows that atomic diffusion is also occurring in the sun and suggest that some weak mixing is also needed in order to account for the small Li abundance (Buldgen et al. 2019 and references therein) and could also have large effects on the pulsational properties of other stars (Turcotte et al. 2000, Vauclair & Théado 2004, Théado et al. 2005, Hu et al. 2011, Deal et al. 2017).

## 2 Atomic diffusion and opacities

A convenient way to express the diffusion velocity is to consider a ternary mixture (Aller & Chapman 1960) and add radiative acceleration, $g_{rad,i}$, as introduced by Michaud (1970). For an element $i$ it could be written in a schematic expression like

$$V_{D,i} \propto D_{ip}\left[A_i \frac{m_p}{kT}(g_{rad,i} - g) + ...\right],$$

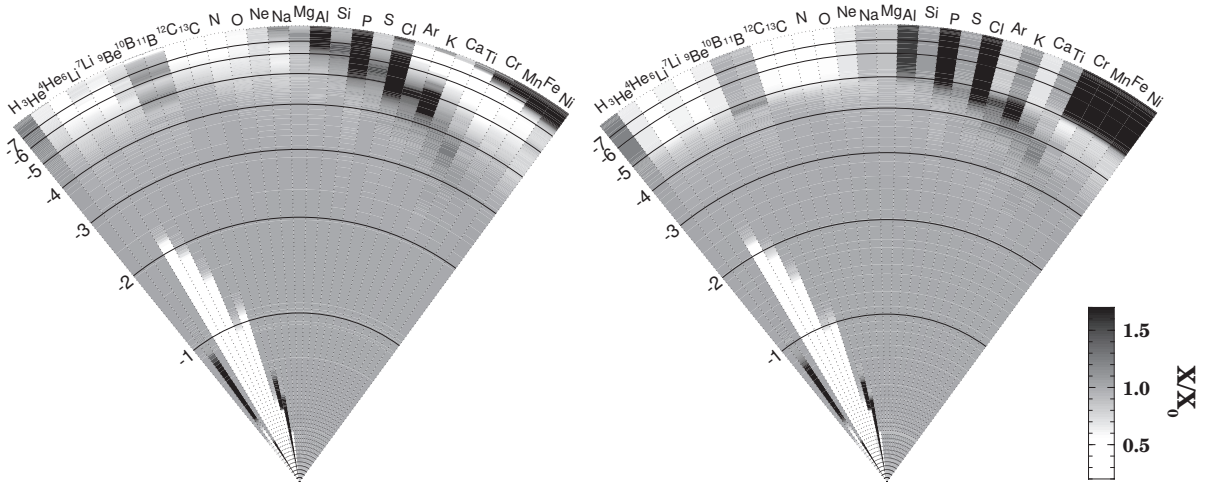


Figure 1: Abundance profiles inside two $2.5\ M_{\odot}$ stars at 500 Myrs that show similar surface abundances. The model with atomic diffusion and mass loss is shown in the left panel (mass loss rate of $10^{-13} M_{\odot}\mathrm{yr}^{-1}$) and the model with atomic diffusion and turbulent mixing (T5.2D1M-4) is shown in the right panel (see Vick et al. 2010 for more details). The concentration is grey coded with a contrast identified in the right insert. The scale is linear in radius with the corresponding $\log(\Delta M/M_{*})$ given on the left-hand side.

where $D_{ip}$ is the atomic diffusion coefficient and the terms represented by "+..." are generally smaller contributions due to the thermal diffusion and to the purely diffusive term. This expression clearly shows the competition between gravity and radiative acceleration. This competition will lead to chemical stratification in radiative zones of stars as shown in Figure 1.

The radiative acceleration of the element $i$, at large optical depth, may be approximated by:

$$g_{rad,i}(r) \propto \frac{L^{rad}(r)\kappa_R}{X_i} \int_0^{\infty} \frac{\kappa_u(i)}{\kappa_u(\mathrm{total})} P(u)du,$$

where $r$ is the radius, $X_i$ is the mass fraction of the element $i$, $L^{rad}(r)$ is the radiative luminosity, $\kappa_R$ is the Rosseland opacity, $\kappa_u(i)$ and $\kappa_u(\mathrm{total})$ are respectively the contribution to the opacity of the element $i$ and the total opacity at the frequency $u = h\nu/kT$, and $P(u)$ is the normalised black body flux distribution. The value of $g_{rad,i}(r)$ depends on the competition between element $i$ and the other elements to interact with the photons. It also shows that radiative acceleration will become large in the region where the element $i$ become a strong contributor to the opacity, so the radiative acceleration and the opacity are strongly linked (Richard et al. 2001, Alecian et al. 2009, Hui-Bon-Hoa & Vauclair 2018, Hui-Bon-Hoa et al. 2018).

Figure 2 shows the contribution to the Rosseland opacity of different chemical elements in a $1.5\ M_{\odot}$ around 200000 K early in the evolution, before large changes in the chemical composition, and at approximately the age of the Hyades (670 Myr). At this temperature, even for the original composition before the accumulation of iron due to strong radiative acceleration, the removal of the Fe contribution to the opacity reduces the Rosseland opacity by a factor of 2, showing that it is a major contributor at that temperature. Removing other species like O or Ni reduces the Rosseland opacity by a factor of 1.1 or more. Later in the evolution, iron-peak elements have increased while others have decreased at this temperature, which increases the contribution to the Rosseland opacity of the iron-peak elements. Removing Fe and Ni then reduces the Rosseland opacity by a factor of 4 and 1.4 respectively.

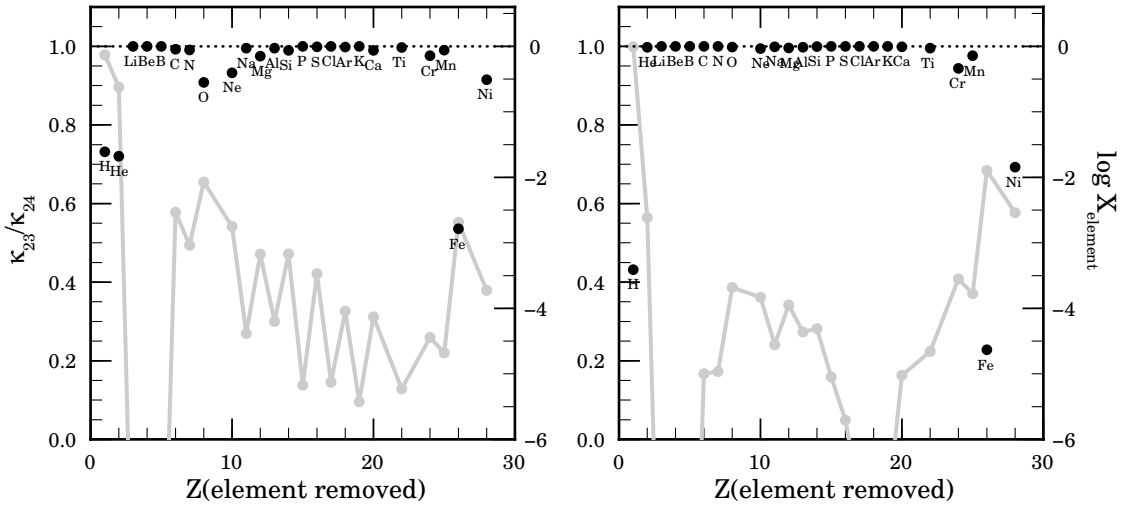


Figure 2: Ratio of the Rosseland opacity evaluated without including the spectrum of the element of atomic number Z, and of that obtained with the complete mixture (24 elements). The gray curves give the local element abundances at that time. Calculations were done at 200000 K in a $1.5\ M_{\odot}$. Left panel: Close to starting composition (30 Myr), Right panel: after some 670 Myr of evolution (see Richard et al. 2001 for details).

# 3 Impact of atomic diffusion in stellar structure and evolution

Atomic diffusion occurs in stars from the surface to the center and even if these effects are reduced in the external layers by other transport processes it remains in the center. In low metallicity stars, VandenBerg et al. (2002) have studied the effect of the atomic diffusion on globular clusters age determination, using evolutionary track of models computed by Richard et al. (2002). Figure 3 shows the fit of the M 92 fiducial to the field subgiant HD 140283 (Stetson & Harris 1988) with the isochrones calculated for models without atomic diffusion (left panel) and models with atomic diffusion and a small turbulence, which reduces the effect of atomic diffusion in the external layer to reproduce the Lithium plateau. In the two panels, four isochrones are plotted: 12 Gyr, 14 Gyr, 16 Gyr, and 18 Gyr. VandenBerg et al. (2002) found an age of 13.5 Gyr for M 92, presumably one of the oldest globular clusters of the Galaxy, which is ∼2.0 Gyr less than had been obtained in the absence of atomic diffusion by Grundahl et al. (2000). This reduction in the age determination of globular clusters is mainly due to the diffusion of helium in the central region of the star and is independent of the turbulence in the outer regions. Atomic diffusion also leads to abundance gradients of heavy elements in the centre of the star as shown in Figure 5 of Richard et al. (2002).

Michaud et al. (2004) have computed self-consistent stellar models including atomic diffusion to study M 67 and NGC 188 stars . They found that no convective core overshooting is required to fit the turnoff morphology including the luminosity gap in M 67, and determined ages of 3.7 Gyr and 6.7 Gyr for M 67 and NGC 188 respectively, which are younger by about 3% and 7% respectively than the ages obtained using models computed without atomic diffusion. The effect of the enhancement of helium and heavy elements abundances in the central region of these models due to atomic diffusion is illustrated in Figure 4. The left, center, and right panel show respectively the evolution of effective temperature, of the depth of the surface convective zone, and of the mass of the convective core for a set of models computed without atomic diffusion (grey lines) and a set computed with atomic diffusion (black lines). The right panel clearly shows the effect of atomic diffusion on the convective core. The convective core appears in less massive stars in models including atomic diffusion (around $1.095\ M_{\odot}$) than in models without atomic diffusion for which the convective core appears in models

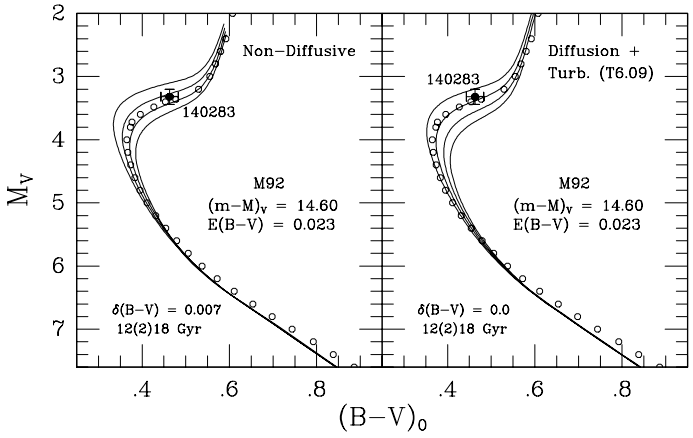


Figure 3: Fit of the M 92 fiducial to the field subgiant HD 140283 (Stetson & Harris 1988). Isochrones were calculated for models without atomic diffusion (left panel) and models with atomic diffusion and turbulence (right panel, see VandenBerg et al. 2002 for details).

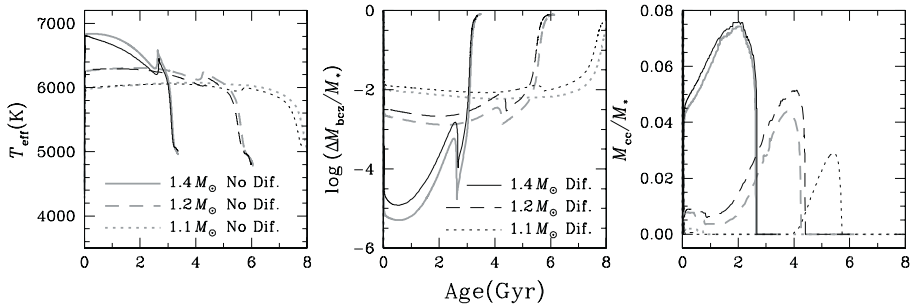


Figure 4: Left, center, and right panel show respectively the evolution of the effective temperature, of the depth of the surface convective zone, and of the mass of the convective core. Models computed without atomic diffusion are plotted in gray and those computed with atomic diffusion are plotted in black.

with a mass greater than $1.14\ M_{\odot}$. While in $1.2\ M_{\odot}$ and $1.3\ M_{\odot}$ models, diffusion increases the convective core size by about 20% and 10% respectively, the size of the convective core in the $1.4\ M_{\odot}$ models is very similar with and without atomic diffusion. New observations of M67 open clusters seem to indicate that atomic diffusion is at work in stars of this cluster (Bertelli Motta et al. 2018, Souto et al. 2018).

More massive models for A and F stars show an opacity increase around 200000K due to the iron-peak elements accumulation caused by radiative accelerations (Turcotte et al. 1998, Richer et al. 2000), when macroscopic motions are not rapid enough to wipe out their effect, and could lead to the appearance of an iron convective zone. These iron convection zones have been studied by Richard et al. (2001) for B, A and F stars. They found that, at solar metallicity, the iron convection zones naturally appear under the surface convective zone for stars more massive than $1.5\ M_{\odot}$. We can see in Figure 5 that as the mass of the star increases the iron convection zone appears earlier during the evolution and is present until the surface convective zone starts to decrease on the subgiant branch. Before the appearance of the iron convective zone, the heavy elements accumulation could lead to an inverse mean molecular gradients and to successive episodes of double diffusive convection as shown by Théado et al. (2009), Vauclair & Théado (2012), Deal et al. (2016).

However, only considering atomic diffusion without competing transport processes of chemical species often leads to predicted abundance anomalies greater than the anomalies obtained from obser-

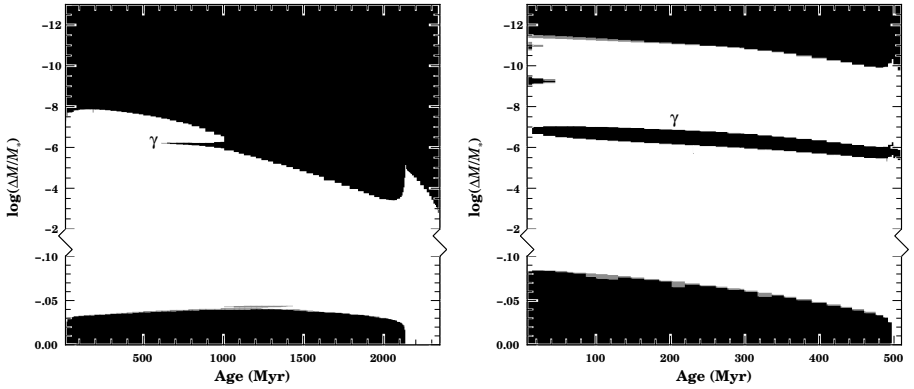


Figure 5: The evolution of the convective zones is shown in the left panel for a $1.5\ M_{\odot}$ model and in the right panel for a $2.5\ M_{\odot}$ (black zones are convective regions, white zones are radiative regions, and grey zones are semi-convective regions). The iron convective zone is labelled $\gamma$.

vations. In order to quantitatively reproduce observed surface abundances in AmFm stars, Richer et al. (2000) have included turbulent mixing in stellar evolutionary models with atomic diffusion. They are able to reproduce the observed surface abundances for many AmFm stars of many open clusters. Similar models have also successfully explained observed abundances in metal poor stars (Richard et al. 2005, Korn et al. 2006, 2007, Nordlander et al. 2012, Gruyters et al. 2013) and in horizontal branch stars (Michaud et al. 2007, 2008, 2011a). Nonetheless, other studies in static models have suggested that mass loss could also reduce the predicted abundance anomalies to observed levels (Michaud et al. 1983, Michaud & Charland, 1986, Alecian 1996). Recently self-consistent evolutionary models including both atomic diffusion and mass loss have been computed for a large variety of stars at different evolutionary stages and for different metallicities. Vick et al. (2010) have computed the first self-consistent evolutionary models including both atomic diffusion and unseparated mass loss. They have shown that if mass loss is assumed to be the only transport process competing with atomic diffusion, observed abundance anomalies from open cluster stars as well as Sirius A and $o$ Leonis constrain mass loss rates to 2–5 times the solar mass loss rate. As elemental separation occurs at the same depth in models involving mass loss (Vick et al. 2010) or turbulence (Richer et al. 2000), both these processes in the presence of atomic diffusion are able to explain abundance anomalies obtained from observations of AmFm stars. However, as shown in Figure 1, even if the models with mass loss and with turbulence show similar surface abundances, the internal distribution of elements are different for most elements in the outer 25% of the radius. For example, in the interval of $\log(\Delta M/M_{*}) \simeq -6$ to $-5$ the Fe abundance is 4–5 times greater in the turbulence model than in the model with mass loss. These differences in abundances have an important effect on the local Rosseland opacity, which could lead to different asteroseismic properties for the two models. These different internal abundance profiles will also lead to different surface abundance variations during the sub-giant branch phase. New observations of Landstreet (2011) have led Michaud et al. (2011b) to make a detailed analysis of Sirius A. Most of the surface abundances obtained from observations could be well reproduced with a mixed mass of $\sim 10^{-6} M_{\odot}$ (for models with turbulence) or with a mass loss rate of $\sim 10^{-13} M_{\odot}\mathrm{yr}^{-1}$. They found that surface abundances do not favor mass loss or turbulence as the competing process, but the agreement with the observational determined mass loss rate from Bertin et al. (1995) favors mass loss.

# Acknowledgements

This work was supported by the "Programme National de Physique Stellaire" (PNPS) of CNRS/INSU co-funded by CEA and CNES.


# References


Alecian E., Wade G. A., Catala C. , Bagnulo S., Böhm T., Bouret J.-C., Donati J.-F., Folsom C. P., Grunhut J., and Landstreet J. D. 2009, MNRAS, 400, 354

Alecian G. 1996, A&A, 310, 872

Aller L.H., Chapman S. 1960, ApJ, 132, 461

Bertelli Motta C., Pasquali A., Richer J. et al. 2018, MNRAS, 478, 425

Bertin P., Lamers H. J. G. L. M., Vidal-Madjar A. , Ferlet R., Lallement R. 1995, A&A, 302, 899

Buldgen G., Salmon S. J. A. J., Noels A. et al. 2019, A&A, 621, A33

Chapman S. 1917, MNRAS 77 540

Deal M., Richard O., Vauclair S. 2016, A&A, 589, A140

Deal M., Escobar M. E., Vauclair S. , Vauclair G., Hui-Bon-Hoa A., Richard O. 2017, A&A, 601, A127

Eddington A. S. 1916, MNRAS, 77, 16

Grundahl F., VandenBerg D. A., Bell R. A. , Andersen M. I., Stetson P. B.: 2000, AJ, 120, 1884

Gruyters P., Korn A. J., Richard O. , Grundahl F., Collet R., Mashonkina L. I., Osorio Y., Barklem P. S. 2013, A&A, 555, A31

Hu H., Tout C. A., Glebbeek E., Dupret M.-A. 2011, MNRAS, 418, 195

Hui-Bon-Hoa A., Vauclair S. 2018, A&A, 610, L15

Hui-Bon-Hoa A., Vauclair S., Deal M. 2018, in Proceedings of Workshop on Astrophysical Opacities, Astronomical Society of the Pacific Conference Series, 515, 176

Korn A. J., Grundahl F., Richard O. , Barklem P. S., Mashonkina, L., Collet R., Piskunov N., Gustafsson B. 2006, Nature, 442, 657

Korn A. J., Grundahl F., Richard O. Mashonkina L., Barklem, P. S., Collet R., Gustafsson B., Piskunov, N. 2007, ApJ, 671, 402

Landstreet J. D. 2011, A&A, 528, A132

Michaud G. 1970, ApJ, 160, 641

Michaud G., Vauclair G., Vauclair S. 1983, ApJ, 267, 256

Michaud G., Charland Y. 1986, ApJ, 311, 326

Michaud G., Richard O., Richer J., VandenBerg D. A. 2004, ApJ, 606, 452

Michaud G., Richer J., Richard O. 2007, ApJ, 670, 1178

Michaud G., Richer J., Richard O. 2008, ApJ, 675, 1223

Michaud G., Richer J., Richard O. 2011a, A&A, 529, A60

Michaud G., Richer J., Vick M. 2011b, A&A, 534, A18

Michaud G., Alecian G., Richer J. 2015, Atomic diffusion in stars, Springer International Publishing Switzerland

Nordlander T., Korn A. J., Richard O. , Lind K. 2012, ApJ, 753, 48

Richard O., Michaud G., Richer J. 2001, ApJ, 558, 377

Richard O., Michaud G., Richer J., Turcotte S., Turck-Chieze S., VandenBerg D. A. 2002, ApJ, 568, 979

Richard O., Michaud G., Richer J. 2005, ApJ, 619, 538

Richer J., Michaud G., Turcotte S. 2000, ApJ, 529, 338

Souto D., Cunha K., Smith V. V. et al. 2018, ApJ, 857, 14

Stetson P. B., Harris W. E. 1988, AJ, 96, 909

Théado S., Vauclair S., Castro M., Charpinet S., Dolez N. 2005, A&A, 437, 553

Théado S., Vauclair S., Alecian G. ,Le Blanc F. 2009, ApJ, 704, 1262

Turcotte S., Richer J., Michaud G. 1998, ApJ, 504, 559

Turcotte S., Richer J., Michaud G., Christensen-Dalsgaard J. 2000, A&A, 360, 603

VandenBerg D. A., Richard O., Michaud G., Richer J. 2002, ApJ, 571, 487

Vauclair S., Théado S. 2004, A&A, 425, 179

Vauclair S., Théado S. 2012, ApJ, 753, 49

Vick M., Michaud G., Richer J., Richard O. 2010, A&A, 521, A62